

On-Orbit Test Results from the EO-1 Advanced Land Imager

J.B. Evans, C.J. Digenis, M. D. Gibbs, D.R. Hearn, D.E. Lencioni, J.A. Mendenhall
MIT Lincoln Laboratory
and
R.D. Welsh
NASA Goddard Space Flight Center

ABSTRACT

The Advanced Land Imager (ALI) is the primary instrument flown on the first Earth Observing mission (EO-1), launched on November 21, 2000. It was developed under NASA's New Millennium Program (NMP). The NMP mission objective is to flight-validate advanced technologies that will enable dramatic improvements in performance, cost, mass, and schedule for future, Landsat-like, Earth Science Enterprise instruments. ALI contains a number of innovative features designed to achieve this objective. These include the basic instrument architecture which employs a push-broom data collection mode, a wide field of view optical design, compact multi-spectral detector arrays, non-cryogenic HgCdTe for the short wave infrared bands, silicon carbide optics, and a multi-level solar calibration technique.

During the first ninety days on orbit, the instrument performance was evaluated by collecting several earth scenes and comparing them to identical scenes obtained by landsat7. In addition, various on-orbit calibration techniques were exercised. This paper will present an overview of the EO-1 mission activities during the first ninety days on-orbit, details of the ALI instrument performance and a comparison with the ground calibration measurements.

Keywords: EO-1, performance assessment, radiometric calibration, solar calibration, sensitivity, spatial, Landsat 7

I. INTRODUCTION

The first Earth-Observing satellite (EO-1) in the New Millennium Program (NMP) of the National Aeronautics and Space Administration (NASA), launched on November 21, 2000, carries an Advanced Land Imager (ALI) with multispectral imaging capability^{1,2}. The NMP missions are structured to accelerate the flight validation of advanced and enabling technologies that will enable dramatic improvements in performance, cost, mass, and schedule of future missions. The focus of EO-1 is the validation of technologies relevant to Landsat missions. The ALI has been designed to produce images directly comparable to those from the Enhanced Thematic Mapper Plus (ETM+) of Landsat 7. The EO-1 satellite is in a sun-synchronous, 705 km orbit with a 10:01 AM descending node. Thus, it flies "in formation" with the Landsat 7 satellite, covering the same ground track approximately one minute later than the Landsat 7 satellite. The wavelength limits and ground sampling distances (GSD) of the ALI sensing bands, listed in Table I, are mostly the same as those of ETM+. The exceptions are that the ALI has no band 6 (thermal imaging), the panchromatic (Pan) band has a 10 m, rather than 15 m GSD, and the ALI has three additional bands, 1', 4', and 5'.

2. THE INSTRUMENT

2.1 Instrument Architecture

A conceptual sketch of the ALI illustrating the major design features is shown in Figure 1. The telescope is a f/7.5 reflective triplet design with a 12.5 cm unobscured entrance pupil and a field-of-view (FOV) of 15° cross-track by 1.26° in-track. It

Table 1. Spectral bands of the Advanced Land Imager

Band	Wavelength (μm)	GSD (m)
Pan	0.480-0.690	10
MS-1'	0.433-0.530	30
MS-1	0.450-0.515	30
MS-2	0.525-0.605	30
MS-3	0.630-0.690	30
MS-4	0.775-0.805	30
MS-4'	0.845-0.890	30
MS-5'	1.200-1.300	30
MS-5	1.550-1.750	30
MS-7	2.080-2.350	30

employs reflecting optics throughout, to cover the fullest possible spectral range. At the focal plane, detectors are linearly arrayed in the cross-track direction. As the satellite moves along its track, the image of the ground is recorded in the “push-broom” mode. There are no moving scan mirrors. When not recording an image, a motorized cover closes the entrance aperture of the telescope housing. While the aperture cover is closed, detector dark currents are recorded, and an internal reference lamp assembly illuminates the detectors briefly with one, two, and three lamps to verify consistent operation of the detector system.

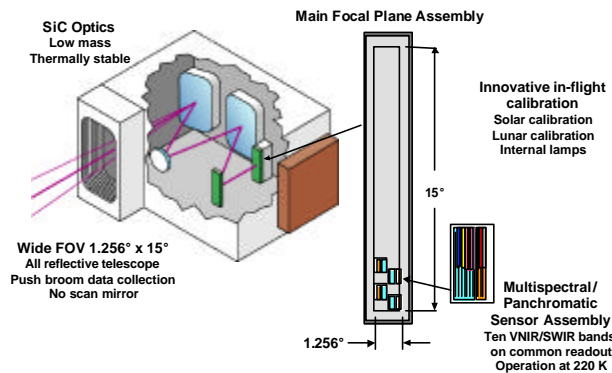


Figure 1: A conceptual sketch of the ALI telescope and Focal Plane Assembly.

2.2 Advanced Technologies

The design of the telescope, with a FOV wide enough to cover the whole 185 km Landsat swath, enables the use of the “push-broom” imaging mode. The optical design features a flat focal plane and telecentric performance, which greatly simplifies the placement of the filter and detector array assemblies. The design incorporates silicon carbide mirrors and an Invar truss structure with appropriate mounting and attachment fittings. Silicon carbide possesses a high stiffness to weight ratio, a high thermal conductivity, and a low coefficient of thermal expansion. NMP Instrument Technology and Architecture team member SSG, Inc. supplied the telescope.

Although the optical system supports a 15° wide FOV, only 3° was populated with four sensor chip assemblies (SCA’s) as illustrated in Figure 2. The Pan detectors subtend 10 m square pixels on the ground and are sampled every 10 m as the earth image moves across the array. The MS detectors subtend 30 m and are sampled every 30 m. Each MS band on each SCA contains 320 detectors in the cross-track direction, while each Pan band contains 960 detectors. The ground swaths of the neighboring SCA’s overlap by 300 m. The total cross-track coverage from the single MS/Pan module is 37.5 km.

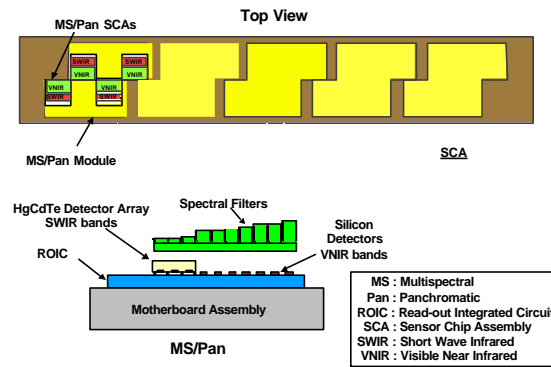


Figure 2. Focal Plane Assembly.

The MS/Pan arrays use Silicon-diode VNIR detectors fabricated in the Silicon substrate of a Readout Integrated Circuit (ROIC). The SWIR detectors are Mercury-Cadmium-Telluride (HgCdTe) photo-diodes that are Indium-bump bonded onto the ROIC that services the VNIR detectors. The nominal focal plane temperature is 220 K and is maintained by the use of a passive radiator and heater controls.

Application of detectors of different materials to a single readout integrated circuit (ROIC) enables a large number of arrays covering a broad spectral range to be placed closely together. This technology is extremely effective when combined with the wide cross-track FOV optical design being used on the ALI.

Both the array frame rate and the detector integration time can be set by commands to the Focal Plane Electronics (FPE). The nominal integration times are 4.05 msec for the MS detectors and 1.35 msec for the Pan. The frame rate can be adjusted in 312.5 nsec increments to synchronize frame rate with ground scan velocity variations due to altitude and velocity variations during orbit. The FPE samples the output of each detector with a 12-bit converter. Predicted signal-to-noise ratios (SNR's) for the ALI are shown in Figure 3. NMP Instrument Technology and Architecture team member Raytheon Systems Santa Barbara Remote Sensing (SBRS) supplied the focal plane system.

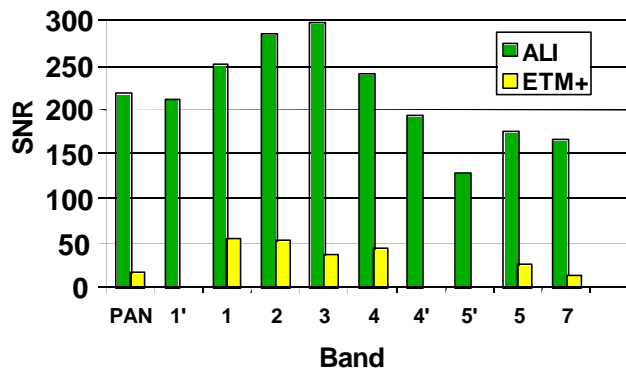


Figure 3. Signal-to-noise ratios of the ALI bands compared with those of ETM+, for a solar zenith angle of 22.5° and 5% surface reflectance.

The ALI employs a novel approach to solar calibration that enables radiometric calibration over the full range of expected earth radiances. This on-orbit solar calibration is one of four independent techniques being used to establish a high confidence radiometric calibration for the ALI³. The three other radiometric calibration techniques are the pre-launch laboratory calibration, lunar scans, and measurements of well-characterized ground scenes^{4,5,6}. For solar calibration there is motor-driven aperture selector in the aperture cover assembly. Just prior to solar calibration, a Spectralon diffuser plate is

swung over the secondary mirror by a motor-driven mechanism. Then the aperture selector moves an opaque slide over a row of small to increasingly larger slit openings and then reverses the slide motion to block all light. In the process, the FPA receives irradiance equivalent to earth-reflected sunlight for an earth albedo ranging from 0 to 100%.

3. PERFORMANCE ASSESSMENT OF INSTRUMENT

The performance assessment plan for the ALI included pre-flight calibration of the instrument, testing of on-orbit functionality, and detailed image analysis of collected data. For the pre-flight calibration, extensive calibration tests were performed before the instrument was integrated with the spacecraft⁷⁻¹⁰. Spectral calibrations were done with monochrometers⁷. Radiometric calibration employed a large integrating sphere and a calibrated reference lamp⁸. Spatial calibrations included knife-edge scans for modulation transfer function, and line-of-sight (LOS) calibrations, both performed with an imaging collimator⁹.

The on-orbit functionality of the Advanced Land Imager includes all aspects of the instrument required to accurately image various Earth scenes: electrical, thermal, commanding, and interfacing with the Wideband Advanced Recorder Processor (WARP) data recorder. Telemetry trending of key instrument voltages and currents indicates the electrical integrity of the instrument has been excellent and well within limits established prior to launch. All temperature sensor readings have been within seven degrees of preflight predictions during normal operating periods, indicating the thermal performance of the instrument is close to preflight expectations. The observed seven-degree offset can be explained by a warmer instrument pallet caused by additional instrument, data recorder, and X-band phased array usage during the first sixty days. The commanding of the instrument has been nominal with zero errors during the first sixty days on orbit. Finally, no errors associated with the ALI and WARP interface have been identified.

Detailed analysis of the data collected on orbit is the final step of validating and assessing the instrument performance, and requires a wide variety of scenes testing the full-dynamic range of the instrument and all new technologies. EO-1 launched November 20, 2001. The first data collected with the ALI was over Sutton, Alaska five days later on November 25, 2001. Due primarily to manpower-related operational constraints, early operations were limited to 4 scene collects a day and slowly grew to 8 scenes a day. To allow for pointing of the instrument and sufficient settling time, scene collects were also limited to one per path. Working within these constraints, scenes were chosen by the three instrument teams involved with the EO-1 program during the first 90 days to meet requirements for performance assessment. A total of 491 scenes at 294 unique sites were collected during this time. And as of June 1, 2001, 1008 scenes of 476 unique sites have been collected and are shown in Figure 4. These scenes included but are not limited to the following types of sites: uniform radiance, known radiance, high albedo, night scenes, geometric supersites, rugged terrain, metropolitan areas, bridges and canals, solar and lunar calibrations. All scenes collected during the day over the continental United States are by default co-collects with Landsat 7 allowing for direct comparisons between the two instruments.

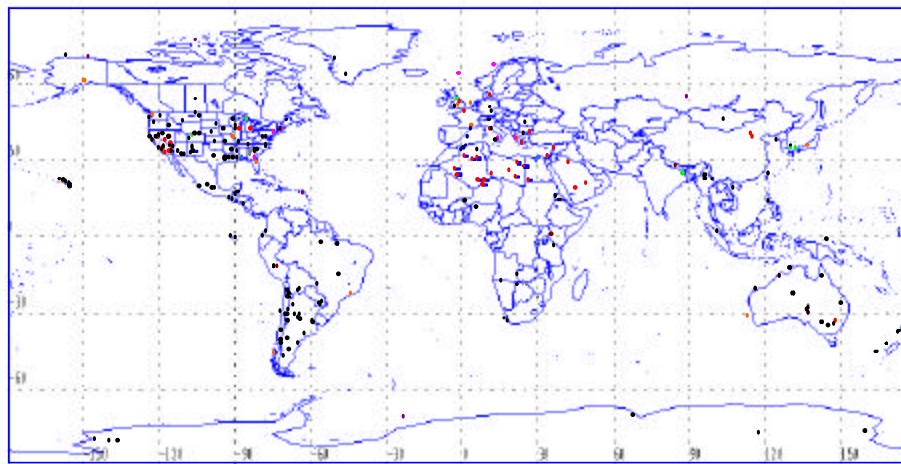
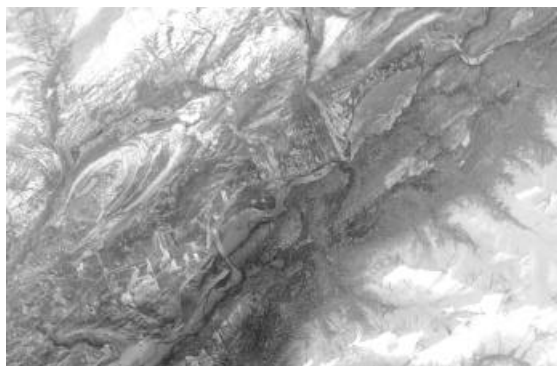


Figure 4. Location of data scenes collected through June 1, 2001.

4. PERFORMANCE ASSESSMENT RESULTS

4.1 Imaging Performance

Initial on-orbit data fulfill expectations for the ALI imaging performance. This is illustrated in Figure 5a, which is the very first image acquired by ALI, a Panchromatic image of Sutton, Alaska. The solar elevation angle was only 5° . The area shown is 19.5 by 12.8 km. A Panchromatic image of a 4.5 km square in the center of Washington, D. C. is seen in Figure 5b.



(a)



(b)

Figure 5a: Panchromatic image of Sutton, Alaska. 5b: Panchromatic image of Washington, D. C.

ALI was designed as a technology demonstration to assure continuity of Landsat data by way of introducing new and improved technologies for future Landsat missions. Figure 6 is a comparison of the Landsat 7 and ALI panchromatic data for the same region of Sutton, Alaska. Notice the improved image quality due to the higher spatial resolution and the improved signal-to-noise ratio of ALI.



(a)



(b)

Figure 6: Comparison of Landsat 7 (a) and ALI (b) panchromatic images.

4.2 Spatial Response

The optical modular transfer function (MTF) is the spatial frequency response commonly used to determine the ability of an instrument to resolve features spatially. In the laboratory the MTF was calculated by scanning a knife edge across the focal plane. On orbit a lunar calibration scan offers a means of testing the optical MTF of the system. The angular speed of the scan was such that the image motion at the focal plane was one-eighth of the normal earth image speed. The Pan image of the first-quarter moon is in Figure 7. We show a plot of the scaled Panchromatic radiance vs. focal plane distance near the moon's limb (symbols in Figure 8) which is an excellent match to an edge-spread function computed from the spatial transfer function derived from our laboratory calibrations (line in Figure 8.)



Figure 7: Panchromatic image from a lunar calibration scan.

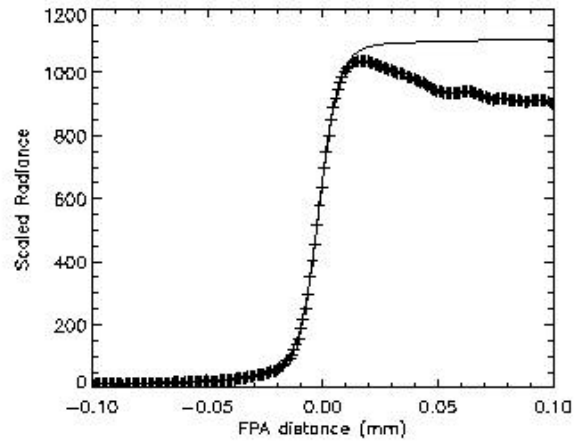


Figure 8: Averaged Panchromatic lunar limb profile from (symbols) compared with an edge-spread function (line) computed with the spatial transfer function from laboratory calibrations.

In addition to the lunar calibration scan, observations of long bridges, dams, canals, and roads can also be used to characterize the system MTF. Work in this area is ongoing.

4.3 Radiometric Response

4.3.1 Saturation Radiance

The ALI was designed such that the focal plane would not saturate for mid-latitude summer scenes with 100% Earth equivalent albedo. These high saturation radiances will allow for the direct observation of clouds, snowfields, frozen rivers, and glaciers.

The saturation radiances of the ALI have been checked on orbit by observing scenes with high albedo. Figure 9a depicts a Band 4,3,2 ALI observation of Hawaii, HI under partially cloudy skies. Figure 9b depicts a Band 4,3,2 image of East Antarctica. In each observation the high albedo regions are clearly resolved and not saturated. Table 2 lists the maximum radiance and number of counts in each band for each scene.

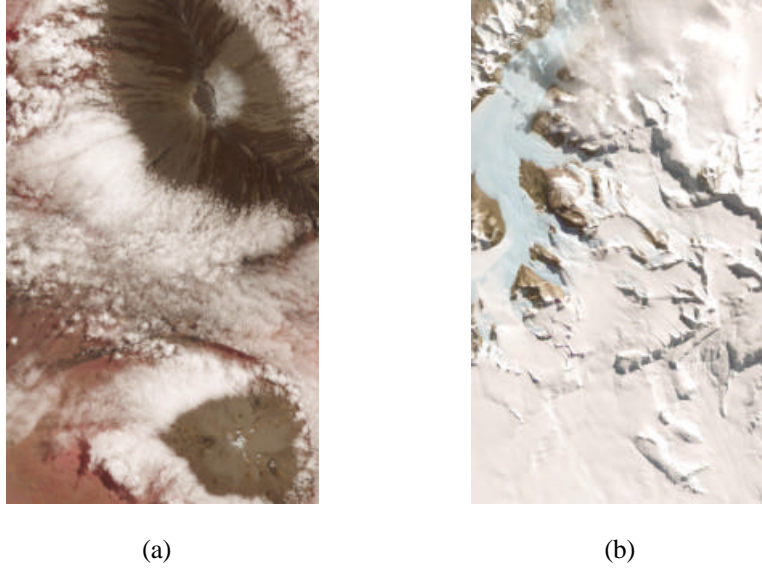


Figure 9a: Band 4,3,2 image of Hawaii, HI. b: Band 4,3,2 image of East Antarctica.

Table 2. Response of ALI to high albedo scenes.

Band	Hawaii HI (Clouds)		East Antarctica (Ice)	
	Radiance (mW/cm ² sr ⁻¹)	Counts ¹	Radiance (mW/cm ² sr ⁻¹)	Counts ¹
1p	24.52	1017	15.16	619
1	30.44	1189	18.25	705
2	28.36	1630	15.97	939
3	25.03	2052	13.71	1182
4	20.83	2705	10.68	1424
4p	17.83	2769	8.82	1423
5p	7.92	1492	1.85	342
5	3.43	1573	0.18	82
7	0.76	1246	0.043	72
Pan	27.67	1797	15.19	980

¹=Maximum counts = 4095

4.3.2 Sensitivity

The sensitivity of the ALI has been demonstrated by imaging several cities at night. Figure 10 depicts a panchromatic image of Las Vegas at night on January 22, 2001. Clearly visible are lights from various hotels and casinos. This scene demonstrates the ALI is capable of detecting events with radiances of 0.033 mW/cm² sr⁻¹ for this band. Table 3 lists the sensitivities of each band, as determined from this image.

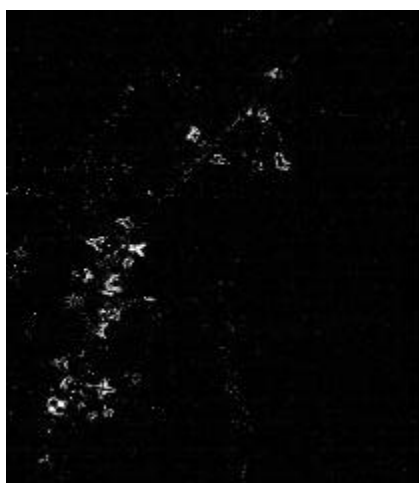


Figure 10: Panchromatic image of Las Vegas at night.

Table 3. ALI Sensitivity

Band	Radiance (mW/cm ² sr ì)
1p	0.067
1	0.067
2	0.067
3	0.033
4	0.013
4p	0.013
5p	0.100
5	0.033
7	0.013
Pan	0.033

4.3.3 Signal to Noise Ratio

The focal plane of the ALI has been designed to provide a signal-to-noise ratio for each band between four and ten times that of the Landsat ETM+. To check signal to noise ratios on-orbit, we have selected three regions of a data set, collected as a part of the on-orbit solar calibration sequence³, representing low, medium, and high albedo scenes. Initially, this data is radiometrically calibrated using calibration coefficients derived during ground testing of the instrument at Lincoln Laboratory. Next, regions of constant radiance are identified. The signal to noise ratio for each region is then calculated for each band. Table 4 lists the derived signal to noise ratios for all bands.

Table 4. Signal to noise ratio for varying radiances.

Band	Radiance*	SNR	Radiance*	SNR	Radiance*	SNR
1p	4.78	151	14.79	339	34.92	520
1	5.55	245	17.08	572	41.1	1263
2	5.11	310	16.10	1001	38.28	1536
3	4.29	343	13.37	1039	31.99	1933
4	3.34	358	10.44	722	25.03	1123
4p	2.80	350	8.73	710	20.93	1145
5p	1.40	263	4.42	662	10.66	1258
5	0.68	341	2.15	1040	5.13	1606
7	0.22	274	0.68	912	1.63	1636
Pan	4.82	215	15.04	348	36.01	703

* mW/cm² sr ì

4.3.4 Absolute Radiometry

Four methods are used to determine the absolute radiometric calibration of the Advanced Land Imager: pre-launch laboratory measurements, lunar scans, solar calibration, and measurements of well-characterized ground scenes. Radiometric knowledge of the well-characterized ground scenes comes from field campaigns, underflight measurements by aircraft, intra-satellite comparisons, and use of scenes with established radiance information. In addition, the radiometric stability is monitored with internal calibration lamps. The absolute radiometric accuracy of the Advanced Land Imager is currently under investigation.

A significant problem with contamination build-up on the surface of the filters overlaying the focal plane was identified during the first 40 days on orbit. Since that time, the focal plane has been baked out for a period of twenty hours every seven days. These outgassing periods have been very successful and internal reference lamps, monitored daily, indicate any contaminant build-up between outgassing periods is effectively eliminated by warming the focal plane and the response of the instrument has been stable to within 2% for the ninety days since the outgassing cycle was adopted. -

At the writing of this paper, three field campaigns have been conducted: Lake Frome Australia , Arizario Argentina, and Barreal Blanco Argentina. Additionally, observations of the full Moon and observations of the Sun, using a novel technique, which allows the full dynamic range of the instrument to be calibrated during a single data collection period³, have also been conducted. Unfortunately, the data collected during ground campaigns, and observations of the Moon have only been recently acquired and radiometric results from these investigations are not mature enough to be presented at the time of this writing.

A description of the solar calibration technique, one of the many ALI advanced technologies, and preliminary results follow. The detector response during a solar calibration sequence consists of an approximately linear increase as the motor-driven aperture cover opens with a series of constant responses during those times when the slide passes over a row of small to increasingly larger slit openings. These bars provide a set of seven calibrated response points. When the aperture cover reverses direction and closes, the pattern of response reverses and proceeds back down to zero. Typical examples of detector responses for each of the ten ALI spectral bands are shown in Figure 11.

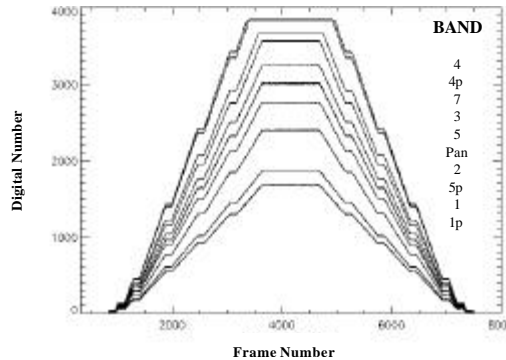


Figure 11. Measured detector responses for the ten ALI bands during a solar calibration.

The flux level at the maximum or seventh level corresponds approximately to a 100% albedo at a 30 degree solar zenith angle. For the data shown, only bands 4 and 4p saturate at this maximum input level. The estimated radiances using the pre-launch calibration for each band are normalized to the expected values from the solar model and are shown in Figure 12. These data are plotted at the mean wavelength of the band. Results for two solar irradiance models (MODTRAN 4.0 – CHKUR model and the World Radiation Center (WRC) model) are shown. Notice the significant differences between the two models in the SWIR region.

With the exception of band 1p, the solar and pre-launch calibrations agree to within the estimated uncertainties of the two independent techniques. The pre-launch calibration accuracy combined with the additional on-orbit effects of contamination and stray light¹¹ is currently estimated to be less than 5% for all bands. The solar calibration uncertainty is currently estimated to be 5% in the VNIR bands and 7% in the SWIR bands. The low response in band 1p is a significant discrepancy between the two calibration techniques. Flight data from the internal reference lamps¹¹ indicate that the on-orbit response of the FPA is consistent with the pre-launch calibration. A potential cause for this result could be degradation of the Spectralon diffuser, which is known to be highly susceptible to contamination. This discrepancy will be resolved by comparing solar calibration results to two other calibration techniques.

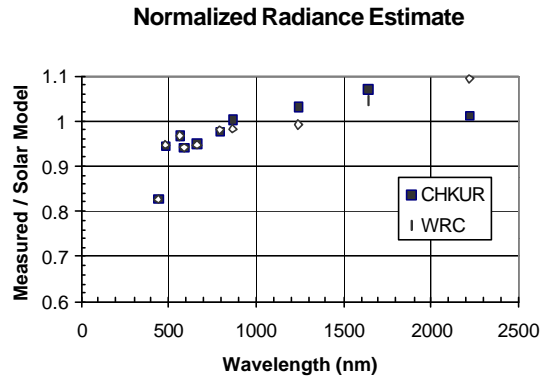


Figure 12. Ratios of measured radiances to calculated radiances from the solar model.

5. CONCLUSION

Initial results from the analysis of data collected by the Earth Observing-1 Advanced Land Imager indicate the instrument is healthy and functioning nominally. The imaging capability has met or exceeded all expectations. The on-orbit spatial performance agrees with the pre-launch prediction. The on-orbit radiometric performance analysis is ongoing with initial results showing focal plane saturation radiances, signal to noise ratios and sensitivities for all bands which equal or better Landsat 7 specifications. This instrument has demonstrated an Advanced Land Imager type instrument would fulfill the requirements for a future Landsat mission with several new technologies to improve the performance and lower the cost of such missions.

REFERENCES

1. J. A. Mendenhall et al., "Earth Observing-1 Advanced Land Imager: Instrument and Flight Operations Overview," MIT/LL Project Report EO-1-1, 23 June 2000.
2. D. E. Lencioni, C. J. Digenis, W. E. Bicknell, D. R. Hearn, J. A. Mendenhall, "Design and Performance of the EO-1 Advanced Land Imager," SPIE Conference on Sensors, Systems, and Next Generation Satellites III, Florence, Italy, 20 September 1999.
3. D. E. Lencioni, J. A. Mendenhall, D. P. Ryan-Howard, "Solar Calibration of the EO-1 Advanced Land Imager," IGARSS, Sydney, Australia, 9 July 2001.
4. J. A. Mendenhall, D. E. Lencioni, A. C. Parker, "Radiometric calibration of the EO-1 Advanced Land Imager," *SPIE Conference on Earth Observing Systems IV*, Denver, Colorado, 18 July 1999.
5. J. A. Mendenhall, D. E. Lencioni, D. R. Hearn, and A. C. Parker, "EO-1 Advanced Land Imager preflight calibration," *Proc. SPIE*, Vol. 3439, pp.390-399, July 1998.
6. J. A. Mendenhall, D. E. Lencioni, D. R. Hearn, and A. C. Parker, "EO-1 Advanced Land Imager in-flight calibration," *Proc. SPIE*, Vol. 3439, pp.416-422, July 1998.
7. J. A. Mendenhall, and A. C. Parker, "Spectral calibration of the EO-1 Advanced Land Imager," *SPIE Conference on Earth Observing Systems IV*, Denver, Colorado, SPIE vol. 3750, July 1999, pp. 109-116.
8. J. A. Mendenhall, D. E. Lencioni, and A. C. Parker, "Radiometric calibration of the EO-1 Advanced Land Imager," *SPIE Conference on Earth Observing Systems IV*, Denver, Colorado, SPIE vol. 3750, July 1999, pp. 117-131.
9. D. R. Hearn, J. A. Mendenhall, and B. C. Willard, "Spatial calibration of the EO-1 Advanced Land Imager," *SPIE Conference on Earth Observing Systems IV*, Denver, Colorado, SPIE vol. 3750, July 1999, pp. 97-108.
10. D. R. Hearn, "Earth Observing-1 Advanced Land Imager: Detector Line-of-Sight Calibration," MIT Lincoln Laboratory Project Report EO-1-4, 29 December 2000.
11. J. A. Mendenhall, D. R. Hearn, J. B. Evans, D. E. Lencioni, C. J. Digenis, R. D. Welsh, "Initial Flight Test Results from the EO-1 Advanced Land Imager: Radiometric Performance," IGARSS International Geoscience and Remote Sensing Symposium, July 2001

This work was sponsored by NASA/Goddard Space Flight Center under U.S. Air Force Contract number F19628-00-C-0002. Opinions, interpretations, conclusions, and recommendations are those of the authors and are not necessarily endorsed by the United States Air Force.

